Developmental Cell
Article

The *C. elegans* SYS-1 Protein Is a Bona Fide β-Catenin

Jing Liu,[1,2] Bryan T. Phillips,[3] Maria F. Amaya,[1] Judith Kimble,[3,4,*] and Wenqing Xu[1,*]
[1]Department of Biological Structure
[2]Biomolecular Structure and Design Program
University of Washington, Seattle, WA 98195-7420, USA
[3]Department of Biochemistry
[4]Howard Hughes Medical Institute
University of Wisconsin-Madison, Madison, WI 53706-1544, USA
*Correspondence: wxu@u.washington.edu (W.X.), jekimble@wisc.edu (J.K.)
DOI 10.1016/j.devcel.2008.02.015

SUMMARY

C. elegans **SYS-1 has key functional characteristics of a canonical β-catenin, but no significant sequence similarity. Here, we report the SYS-1 crystal structure, both on its own and in a complex with POP-1, the *C. elegans* TCF homolog. The two structures possess signature features of canonical β-catenin and the β-catenin/TCF complex that could not be predicted by sequence. Most importantly, SYS-1 bears 12 armadillo repeats and the SYS-1/POP-1 interface is anchored by a conserved salt-bridge, the "charged button." We also modeled structures for three other *C. elegans* β-catenins to predict the molecular basis of their distinct binding properties. Finally, we generated a phylogenetic tree, using the region of highest structural similarity between SYS-1 and β-catenin, and found that SYS-1 clusters robustly within the β-catenin clade. We conclude that the SYS-1 protein belongs to the β-catenin family and suggest that additional divergent β-catenins await discovery.**

INTRODUCTION

β-Catenin is a key regulator of animal development, and defects in its regulation are associated with disease (Giles et al., 2003; Logan and Nusse, 2004; Moon et al., 2002; Moon and Kimelman, 1998; Peifer and Polakis, 2000; Wodarz and Nusse, 1998). In vertebrates and *Drosophila*, a multifunctional β-catenin, the so-called "canonical" β-catenin, acts in the nucleus as a transcriptional regulator for Wnt signaling and in the cytoplasm to mediate cell adhesion (Aberle et al., 1994; van Leeuwen et al., 1994). To accomplish its disparate roles, canonical β-catenin interacts with multiple proteins, including cadherins in the cytoplasm and the TCF DNA-binding protein in the nucleus. No other β-catenin has been identified to date in either vertebrates or *Drosophila* to our knowledge. The *C. elegans* nematode, by contrast, has at least three specialized β-catenins, including BAR-1, HMP-2, and WRM-1 (Korswagen et al., 2000; Natarajan et al., 2001). BAR-1 binds POP-1, the *C. elegans* TCF homolog (Herman, 2001; Lin et al., 1995, 1998), and activates transcription of Wnt signaling target genes (Korswagen et al., 2000). HMP-2 binds cadherin, but not POP-1, and appears specialized for adhesion (Costa et al., 1998; Korswagen et al., 2000; Natarajan et al., 2001), whereas WRM-1 binds and activates Nemo-like kinase to downregulate POP-1 (Thorpe et al., 2000; Rocheleau et al., 1999).

SYS-1 is a fourth potential *C. elegans* β-catenin (Kidd et al., 2005). SYS-1 (for *sy*mmetrical *s*isters) was discovered genetically as a regulator of asymmetric cell division (Miskowski et al., 2001). Normally, certain mother cells divide asymmetrically to generate daughters with distinct fates (e.g., fates A and B); in the absence of SYS-1, the same mother cell instead produces two daughters of one type (e.g., fate A); and with excess SYS-1, it makes two daughters of the opposite type (e.g., fate B). Indeed, SYS-1 controls many asymmetric cell divisions in the *C. elegans* lineage, including EMS, Z1/Z4, and T (Huang et al., 2007; Phillips et al., 2007; Siegfried et al., 2004; Siegfried and Kimble, 2002).

The SYS-1 protein has no significant sequence identity to canonical β-catenins (~9%) and unconvincing sequence identity to other worm β-catenins (~15%) (Kidd et al., 2005). Nonetheless, SYS-1 behaves like a β-catenin in functional assays: SYS-1 acts genetically as a key component of the Wnt signaling pathway; SYS-1 rescues a *bar-1* null mutant when driven by a *bar-1* promoter; SYS-1 interacts with the β-catenin binding domain of POP-1/TCF; SYS-1 acts as a transcriptional coactivator in a TOPFLASH assay in tissue culture cells; and SYS-1 is required for transcriptional activation of the POP-1-dependent promoters of Wnt target genes, which to date include *ceh-22/tinman/NKX2.5* (Lam et al., 2006) and *end-1* (Shetty et al., 2005; Huang et al., 2007).

Although SYS-1 fulfills key functions of a β-catenin, the question remained whether SYS-1 actually belongs to the β-catenin family. To begin to address this question, we solved the SYS-1 crystal structure, both on its own and in a complex with the β-catenin binding domain of POP-1/TCF. We find that the SYS-1 structure, although divergent, has hallmark features of the β-catenin family (e.g., 12 armadillo repeats), and that the SYS-1/POP-1 complex interacts via key features typical of the β-catenin/TCF complex (e.g., the "charged button"). Using our knowledge of SYS-1 structure, we modeled the structures of the three other *C. elegans* β-catenins, and explored how those predicted structures might explain the diversity of their protein binding specificities. Finally, we generated a phylogenetic tree

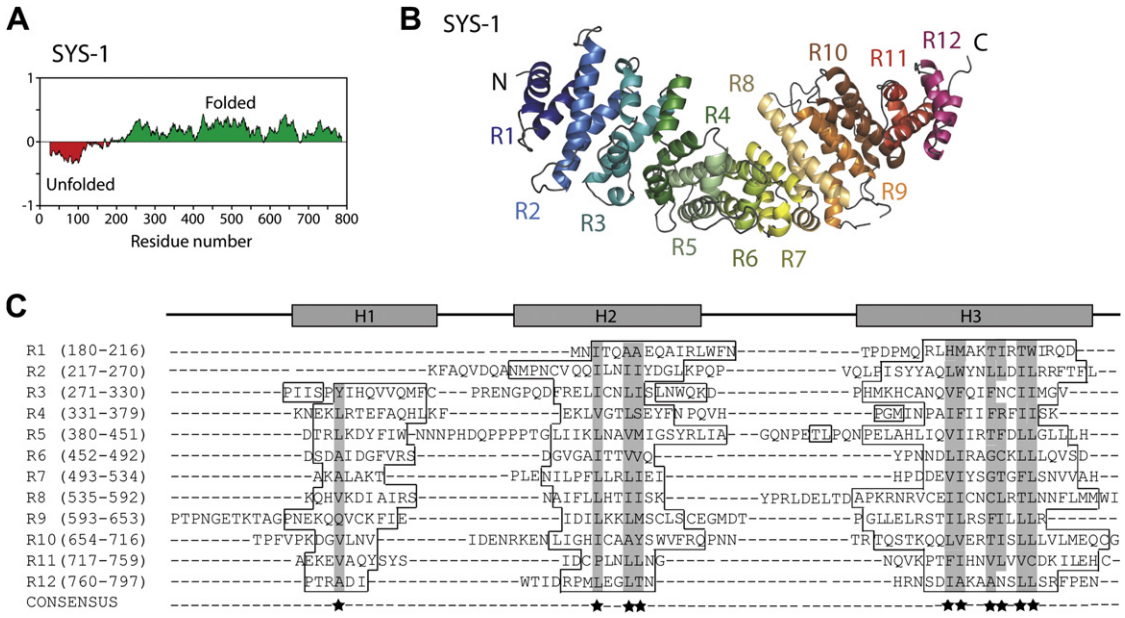

Figure 1. SYS-1 Contains a Domain with 12 Armadillo Repeats

(A) SYS-1 domain structure predicted by FoldIndex. Folded and unfolded regions are colored in green and red, respectively.

(B) Crystal structure of the SYS-1 armadillo repeat region. Each armadillo repeat (R1–R12) is given its own color. N, N terminus; C, C terminus.

(C) Structure-based sequence alignment of the 12 repeats of *C. elegans* SYS-1. Repeat numbers and corresponding amino acids are shown on the left. The specific residues that form helices H1, H2, and H3 are boxed. Structural positions with strong preferences for a given amino acid or group of amino acids are shaded and listed on the line marked "Consensus" with the star symbols.

of β-catenins, focusing on the region most structurally similar between SYS-1 and canonical β-catenin, and found that SYS-1 clusters in the β-catenin clade. We conclude that SYS-1 belongs to the β-catenin family and suggest that features identified here can be used to recognize additional divergent β-catenins.

RESULTS

The SYS-1 Crystal Structure

The SYS-1 protein is composed of two regions (Figure 1A). An N-terminal region of ~180 amino acids is dominated by hydrophilic residues that favor disordered structures (e.g., glycine, proline, and serine) or tend to promote aggregation (poly-Q stretches). Protein sequence analysis by various programs, including FoldIndex, predicted that the SYS-1 N-terminal region is not folded (Figure 1A). It remains unclear whether this N-terminal domain is functionally important. By contrast, the remainder of SYS-1 (residues 180–811) is predicted to be folded (Figure 1A).

We determined the crystal structure of the SYS-1 region containing residues 180–811 at 2.6 Å resolution. Each asymmetric unit in the crystal contained two SYS-1 molecules with essentially identical conformation and with an rmsd of 0.33 Å for all Cα atoms (Table 1). SYS-1(180–811) exists as a monomer in solution (data not shown). The entire SYS-1(180–811) fragment is composed of a single domain with 12 helical repeats (Figure 1B). Each repeat consists of two or three helices that bear hallmark features of classical armadillo repeats (see below). Moreover, each repeat interacts extensively with its neighboring repeats, packing together to form a superhelix with a continuous hydrophobic core. Like canonical β-catenin, the SYS-1 superhelix contains a groove that runs along its surface and that may provide a binding site for its binding partners. For simplicity, we refer to SYS-1(180–811) as the armadillo repeat domain.

Canonical β-catenin is composed of 12 armadillo repeats and flanking N- and C-terminal domains (NTD and CTD), which are unstructured. Both flanking domains are required for transcriptional activation, whereas phosphorylation of the N-terminal domain by GSK-3β and CK1 earmarks β-catenin for degradation by the ubiquitin-proteasome system (Kimelman and Xu, 2006; Polakis, 2002). Based on its crystal structure, the SYS-1 CTD extends beyond the armadillo repeat domain as an unstructured fragment that is much smaller than the CTD of canonical β-catenin. Indeed, the SYS-1 CTD has 16 residues, while that of canonical β-catenin has >100 residues. The lack of any appreciable SYS-1 CTD indicates that SYS-1 uses an alternative mechanism to control transcriptional activity.

Comparison of SYS-1 and Canonical β-Catenin Armadillo Repeat Domains

The SYS-1 armadillo repeat domain shares three major structural features with canonical β-catenins. One common feature is the presence of 12 armadillo repeats (Figures 1B, 1C, 2A, and 2B; Figure S1, see the Supplemental Data available with this article online). This finding is striking, because only three armadillo repeats were predicted from the SYS-1 sequence (Kidd et al., 2005). A second common feature is a superhelix with a groove along its concave surface (Figures 2A and 2C). Moreover, both SYS-1 and canonical β-catenin superhelices are formed by a similar mode of helix-helix packing (see below). The third common feature is the positive charge of the groove (Figure 2C), which is

Table 1. Statistics of Structure Determination of SYS-1 and SYS-1/POP-1 Complex

	SYS-1	SeMet-SYS-1/POP-1
Data Collection		
Space group	C2	P1
Wavelength	0.9796	0.9792
Unit-cell parameters (Å)	a = 203.5, b = 95.05, c = 149.39 α = γ = 90°, β = 127.71°	a = 84.97, b = 85.34, c = 93.67 α = 65.22°, β = 78.08°, γ = 83.02°
Number of molecule/asymmetric unit	2	2
Resolution range (Å)	50.0-2.6 (2.69-2.60)	50.0–2.50 (2.59–2.50)
Completeness (%)	97.5 (91.4)	94.0 (72.8)
Redundancy	3.0	3.7
Unique reflections	70,425	75,516
R_{merge} (%)	6.5 (43.7)	8.2 (26.2)
I/σ(I)	16.1 (2.0)	13.7 (2.2)
Phasing		
Se sites found (expected)		21 (30)
FOM (before/after DM)		0.330 (0.695)
Refinement		
R_{work} (%)	24.5	21.6
R_{free} (%)	28.6	26.1
Overall B-factor	60.5	44.7
Rmsd bond lengths (Å)	0.008	0.009
Rmsd bond angles (°)	1.140	1.155
Ramachandran plot (core, disallowed, %)	93.5, 0.0	94.2, 0.0
The final model		
Number of protein atoms	9771	9888
Number of H_2O molecules	39	72

critical in canonical β-catenins for the TCF/β-catenin interaction (Graham et al., 2000, 2001; Poy et al., 2001). These major structural similarities underscore the functional similarities of the two proteins, as detailed in the Introduction.

We next compared the structures of the armadillo repeat domains of SYS-1 and human β-catenin. Their superposition reveals a reasonable alignment of the N-terminal two-thirds, but a displacement of their C termini by over 25 Å (Figure 2A). Strikingly, in SYS-1, each armadillo repeat is displaced from the superhelix axis, whereas armadillo repeats in β-catenin are roughly located in the superhelix axis (Figure 2A). As a result, the SYS-1 groove is deeper and its superhelix wider than that seen in canonical β-catenin. The SYS-1 superhelix is also arched rather than straight and elongated as in canonical β-catenin (Figure 2A). The more twisted SYS-1 superhelix leaves an open hole in the backbone when viewed down its long axis, a hole that is filled by amino acid main-chain atoms in β-catenin (Figure 2B). Therefore, although the two proteins possess many common features, they are clearly divergent.

To accurately locate the sites responsible for the conformational differences between human β-catenin and SYS-1, we made a pair-wise comparison of their 12 armadillo repeats (Figure S1). Repeats 5–8 in the central region exhibit the least structural change, while the N-terminal and C-terminal repeats have clear differences. One consistent difference is that the SYS-1 armadillo repeats are more variable. In human β-catenin repeats, the size of each helix is roughly the same, with H1, H2, and H3 containing 10–11, 9–12, and 14–16 residues in length, respectively, but the sizes of SYS-1 helices are more variable from repeat to repeat: H1 varies from 7–11, H2 from 9–16, and H3 from 11–24 residues in length (Figure 1C). Indeed, H3 of SYS-1 repeat 8 is almost double the length of the equivalent β-catenin H3. In addition, the loops connecting the helices within each human β-catenin armadillo repeat are 3–5 residues in length (except one long loop in repeat 10), but many loops in SYS-1 loops can extend up to 14 residues. Despite these differences, helix packing within the superhelix is surprisingly consistent in SYS-1 and canonical β-catenin. In both proteins, the ridges formed by every third side chain of one helix are packed into grooves created by every fourth side chain of the next corresponding helix. This "3 in 4" packing produces an average rotation of 30° and 10 Å in translation per repeat in both SYS-1 and β-catenin. The specific residues involved in this packing, however, are poorly conserved.

SYS-1 and β-catenin both form a groove on the concave surface of the superhelix. The H3 helices, which are the most conserved of the three armadillo repeat helices, define both floor and edges of this groove. One common feature of the surface charge distribution within this groove is that both SYS-1 and canonical β-catenin carry a positively charged region that corresponds to the site where POP-1/TCF interacts with repeats 6–9 (Figure 2C). However, outside that region, the surface charge distributions of the two proteins are distinctly different.

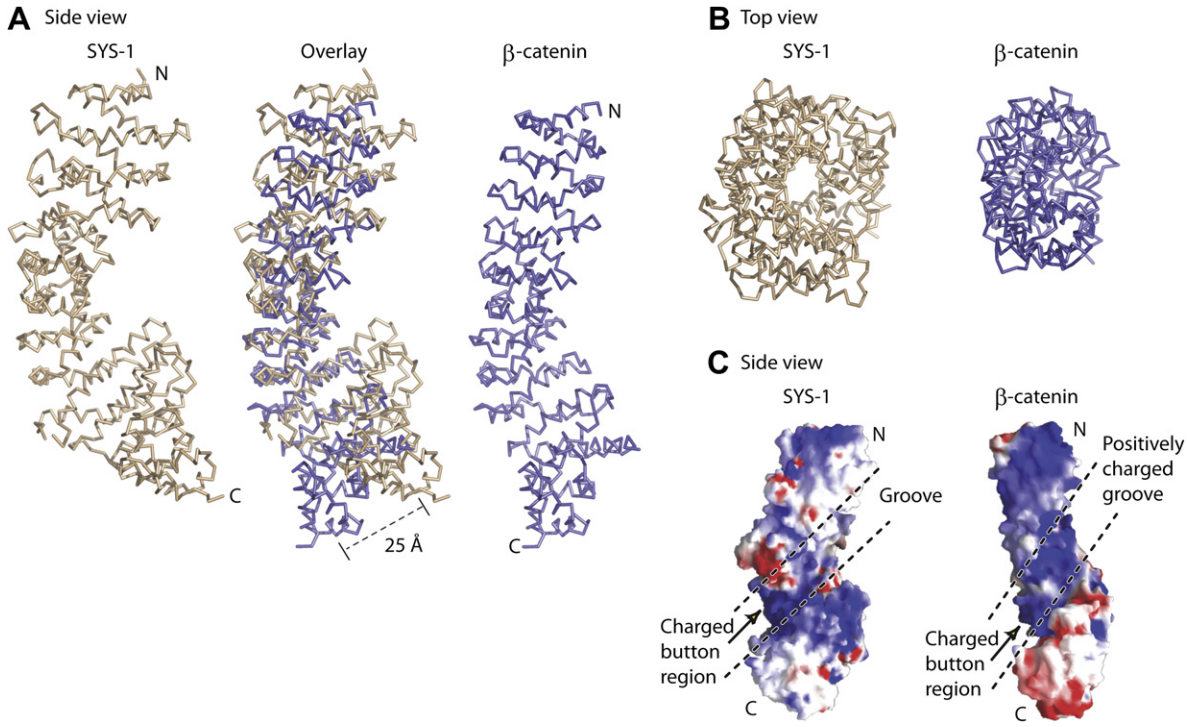

Figure 2. Comparison of Armadillo Repeat Domains in SYS-1 and Human β-Catenin

(A) Superposition of residues 180–811 of SYS-1 (tan) and residues 134–664 of β-catenin (Protein Data Bank ID code: 1G3J, slate) by Pymol. Both proteins are viewed from the side. See Figure S1 for comparisons of individual armadillo repeats.

(B) Top view of SYS-1 (left) and human β-catenin (right). This view is roughly related to that in (A) by a 90° rotation. The deeper groove of SYS-1 creates a hole when viewed from this angle.

(C) Electrostatic surface representation of SYS-1 and β-catenin. Blue represents regions of positive potential and red represents regions of negative potential, at the 10 kT/*e* level. Both SYS-1 and canonical β-catenin carry a positively "charged button" area that is critical for POP-1/TCF binding. While SYS-1 is largely neutral outside of this region, almost the entire β-catenin groove is positively charged. This figure was made with GRASP.

Structural Basis of the SYS-1/POP-1 Interaction

POP-1, the *C. elegans* TCF homolog, is composed of an N-terminal domain bearing sequence similarity to the β-catenin binding domain of human TCF and a central HMG box for DNA binding (Lin et al., 1995; Figures 3A and 3B). Indeed, SYS-1 interacts with the N-terminal 200 residues of POP-1 in a yeast two-hybrid assay (Kidd et al., 2005). We determined the crystal structure of SYS-1(180–811) complexed with POP-1(1–200) at 2.5 Å resolution (Table 1). Two SYS-1/POP-1 complexes with essentially identical conformations reside within each asymmetric unit in the crystal. SYS-1 exhibits little conformational change upon POP-1 binding: the rmsd between bound SYS-1 and unbound SYS-1 is 0.395 Å. For POP-1, electron density was only observed for POP-1 residues 7–14 (Figure 4A), even though the POP-1(1–200) fragment was intact in the crystal as confirmed by an SDS-PAGE gel of the washed and dissolved crystals (data not shown). Therefore, POP-1(7–14) appears to provide the core SYS-1-binding region. Furthermore, an in vitro binding assay with the purified POP-1(1–45) fragment demonstrated that the first 45 residues of POP-1 are sufficient for the SYS-1/POP-1 interaction (Figure 4D). These results indicate that the rest of the POP-1(1–200) fragment does not contain a globularly folded structure and does not make a major contribution to the SYS-1/POP-1 interaction.

POP-1(7–14) adopts an extended strand conformation that runs along the positively charged SYS-1 groove (Figure 3C). When the SYS-1(452–591)/POP-1(7–14) and β-catenin(350–473)/TCF(15–22) complexes were superimposed, the structure of their interactions was almost identical (rmsd = 1.46 Å, Figure 4B). Specifically, in the position equivalent to the salt bridge formed between human TCF D16 and human β-catenin K435, the side chain of POP-1 D8 forms a salt bridge with the side chain of SYS-1 K539. For β-catenin/TCF, this salt bridge between the TCF aspartate and β-catenin lysine is by far the most critical hot-spot for binding and was therefore termed the "charged button" (Graham et al., 2000, 2001; Poy et al., 2001). Interestingly, the *pop-1(q645)* mutation causes a D8E amino acid change in POP-1; this mutant has a fully penetrant Sys defect and the POP-1(q645) protein fails to bind SYS-1 in a yeast two-hybrid assay (Siegfried and Kimble, 2002). To test the importance of the POP-1 D8 to SYS-1 K538 salt bridge, we assayed the ability of purified GST-tagged POP-1 fragments to pull down SYS-1, using both wild-type and mutant forms of each protein. Indeed, although wild-type SYS-1 and POP-1 interacted well (Figure 4D, lanes 3 and 4), either the SYS-1(K539A) or POP-1(D8E) mutation completely abolished the SYS-1/POP-1 interaction (Figure 4D, lanes 5 and 6). We conclude that the salt bridge between SYS-1 K539 and POP-1 D8 functions as a "charged button" for the SYS-1/POP-1 interaction and has been preserved during evolution.

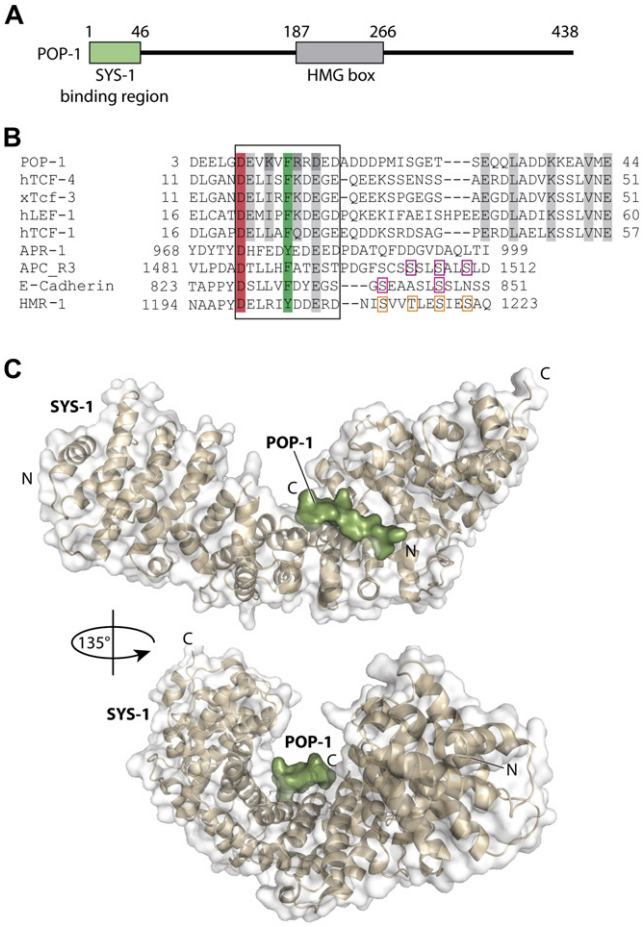

Figure 3. Structure of the SYS-1/POP-1 Complex

(A) POP-1 protein has an N-terminal domain (green) that binds SYS-1 and a central domain (gray) that binds DNA.

(B) Sequence alignment of β-catenin-binding domains that reside within a variety of β-catenin binding partners: *C. elegans* POP-1, human Tcf-4, *Xenopus* Tcf-3, human LEF-1, human Tcf-1, human APC (20 aa repeat 3; APC-R3), human E-cadherin, *C. elegans* HMR-1 (cadherin analog) and *C. elegans* APR-1 (APC analog). Framed by a rectangle is the conserved $Dx\theta\theta x\Phi x_{2\text{-}7}E$ motif (θ and Φ are hydrophobic and aromatic residues, respectively), which is critical for the recognition of β-catenin repeats 5–9. The critical "charged button" and the conserved F/Y residues are colored in red and green, respectively. Other key residues involved in β-catenin binding interactions are also shaded. Critical phosphorylation sites observed in β-catenin/APC and β-catenin/E-cadherin crystal structures are framed in pink. Proposed HMR-1 phosphorylation sites are framed in beige.

(C) Overall structure of the SYS-1/POP-1 complex. SYS-1(180–811) and POP-1(7–14) are in tan and green, respectively. Top view of SYS-1 corresponds roughly to that in Figure 2A. Bottom view shows the shape of the groove that holds POP-1.

In addition to the overall binding mode and critical "charged button," one other important feature is also preserved at the SYS-1/POP-1 interface, the interaction between SYS-1 and POP-1 F13 (corresponding to human TCF4 F21; Figure 4C). Indeed, in the β-catenin/TCF interface, TCF F21 provides one of the most critical residues other than D16 (Gail et al., 2005; von Kries et al., 2000). Beyond D8 and F13, POP-1 seemed to use different amino acids to bind SYS-1. For example, while the E24 of *Xenopus* Tcf3 forms a salt bridge with β-catenin K312, the equivalent POP-1 residue D16 is not observed in the structure to make a salt bridge with K384, the corresponding residue in SYS-1. In addition, K11 in POP-1, which is an Ile or Leu in Tcf/Lef-1 proteins (Figure 3B), forms a salt bridge with E638 of SYS-1; and POP-1 R14 interacts with SYS-1 D492. Neither interaction occurs in the β-catenin/TCF interface (Graham et al., 2000, 2001; Poy et al., 2001). We conclude that the SYS-1/POP-1 interface is anchored by a conserved salt bridge and other species-specific salt bridges.

Modeling Other *C. elegans* β-Catenins

We next modeled the BAR-1, HMP-2, and WRM-1 armadillo repeat domains, using the equivalent regions of either human β-catenin or SYS-1 as a template. The BAR-1 and HMP-2 domains share 48.6% and 52.1% sequence similarity with human β-catenin, respectively (Figure S2A), so we modeled their structures using canonical β-catenin. The WRM-1 armadillo repeat domain shares little overall sequence identity with either human β-catenin or SYS-1, but a small region corresponding to repeats 6–8, WRM-1(418–548) and SYS-1(458–587), is 44.6% sequence similar (Figure S2A), so we modeled WRM-1 from the SYS-1 crystal structure. The BAR-1, HMP-2, and WRM-1 models all contain 12 armadillo repeats (Figure S2B) and a positively charged groove at R7–R9. Moreover, all three contain a lysine in the "charged button" position equivalent to human β-catenin K435 or SYS-1 K539 (K414, K365, and K497 for BAR-1, HMP-2, and WRM-1, respectively; Table S1). Therefore, these three contain hallmark β-catenin features, as expected.

We next asked if the structural models were useful for understanding the differential binding specificity of the various β-catenins toward POP-1. The predicted BAR-1 groove surface is very similar to that of human β-catenin, suggesting that the BAR-1/POP-1 interactions are similar to those of human β-catenin/TCF (Table S1). WRM-1 is predicted to share structural similarities with SYS-1 around the critical K539 "charged button" in armadillo repeat 8 (R8), but WRM-1 does not interact with POP-1 (Korswagen et al., 2000). Our structural model provides an explanation. Among the three key residues surrounding SYS-1 K539 (corresponding to WRM-1 residue K497 in our model), H534 and N586 of SYS-1 are aligned well with the spatially conserved WRM-1 H492 and N547 (Figure 5A). The third SYS-1 residue, A533, corresponds to WRM-1 L491 (Figure 5B). While SYS-1 A533 is close to the POP-1 residue E9 (Figure 5C), the bulky side chain of WRM-1 L491 is predicted to clash with that of POP-1 E9 and thus interfere with the WRM-1/POP-1 interaction (Figure 5D). Consistent with this hypothesis, a SYS-1 A533L mutation abolished the interaction between POP-1 and SYS-1 (Figure 4D, lane 7). It remains unclear why HMP-2 does not bind POP-1, but that may partly be caused by a compromised "charged button" that results from the small HMP-2 A403 side chain. Corresponding residues in other β-catenins are larger than Ala and help stabilize the salt bridge (Table S1). In addition to POP-1 binding, our structural models also provide a basis for understanding partner-binding specificities of the four different functional β-catenins in *C. elegans* (see the Discussion).

SYS-1 Clusters with β-Catenin Phylogenetically

Within the SYS-1 crystal structure, armadillo repeats 6–8 align best with the equivalent armadillo repeats of canonical

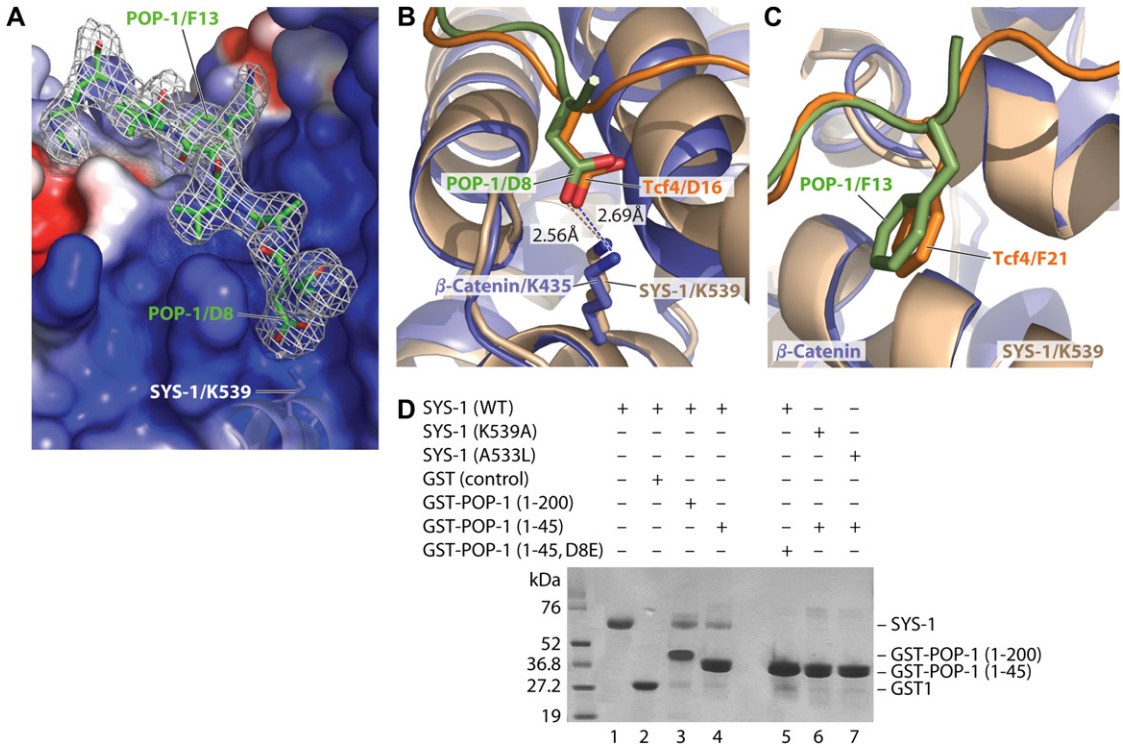

Figure 4. Crystal Structure of SYS-1/POP-1 Complex Reveals the Evolutionarily Conserved "Charged Button"

(A) Representative region of the experimental electron density map of POP-1. The map was subjected to phase extension and density modification at 2.5 Å and contoured at 1 σ. SYS-1 is shown in electrostatic potential surface diagram. POP-1(7–14) is shown in green sticks.

(B) Comparison of the "charged button" regions between the SYS-1/POP-1 and β-catenin/hTcf-4 complexes. The structures of these two complexes were superimposed.

(C) Comparison of a critical hydrophobic interaction that is also evolutionarily conserved.

(D) Association of SYS-1 with POP-1. Lanes 1-4: GST (control), POP-1(1–200) and POP-1(1–45) tagged with GST were tested for the ability to bind wild-type SYS-1 (wt). Lanes 5–7: GST tagged POP-1(1–45) mutant (D8E), and SYS-1 containing point mutations in residues predicted to be important for interacting with POP-1 (K539A and A533L) were tested for interaction. GST-POP-1(1–45) was sufficient to interact with SYS-1 (Lane 4), but POP-1(D8E), SYS-1(K539A), and SYS-1(A533L) all abolished the SYS-1/POP-1 interactions (Lanes 5–7).

β-catenins. Moreover, this region has reasonable sequence similarity with an equivalent region of WRM-1/β-catenin (Figure S2A). We therefore used the amino acid sequences of armadillo repeats 6–8 from several armadillo repeat proteins to construct an unrooted neighbor-joining tree and explore the phylogenetic relationship between SYS-1 and canonical β-catenins. Specifically, we used the sequences of repeats 6–8 from all four *C. elegans* β-catenins, human β-catenin, and *C. elegans* importin-α; repeats 6–8 from human importin-α2 served as an outgroup. SYS-1 grouped robustly with the five β-catenins, while both *C. elegans* importin-α proteins, IMA-2 and IMA-3, fell outside the β-catenin clade (Figure 6). Within the β-catenin cluster, SYS-1 and WRM-1 were most divergent, consistent with their greater sequence differences from human β-catenin. We conclude that SYS-1 groups phylogenetically with other β-catenins rather than with more distantly related ARM proteins.

DISCUSSION

This work presents the crystal structures of SYS-1 and a complex consisting of SYS-1 and its binding partner POP-1. We also model the structures of three other *C. elegans* β-catenins, each with distinct binding properties, and analyze the β-catenin family phylogenetically. Our work supports two major conclusions. First, the SYS-1 protein is a divergent β-catenin, despite its lack of sequence similarity with canonical members of the β-catenin family. This finding is important because it shows that sequence alone is not a sufficient method to identify the full complement of β-catenins encoded by a genome. Second, related β-catenins can possess subtle changes that have major effects on their binding properties and thus major consequences for their function.

SYS-1 Is a Highly Divergent Member of the β-Catenin Family

SYS-1 lacks any significant sequence similarity with canonical β-catenins, but it functions like a β-catenin in several ways (Kidd et al., 2005; see the Introduction). To ask if SYS-1 might be related structurally to canonical β-catenins, we solved its crystal structure, both on its own and in a complex with POP-1, the *C. elegans* TCF homolog. The SYS-1 structure, which is nearly identical in these two crystals, reveals a remarkable similarity to canonical β-catenins, although it is clearly divergent. Several hallmark features stand out as common in both SYS-1 and canonical β-catenins. SYS-1 possesses 12 helical repeats

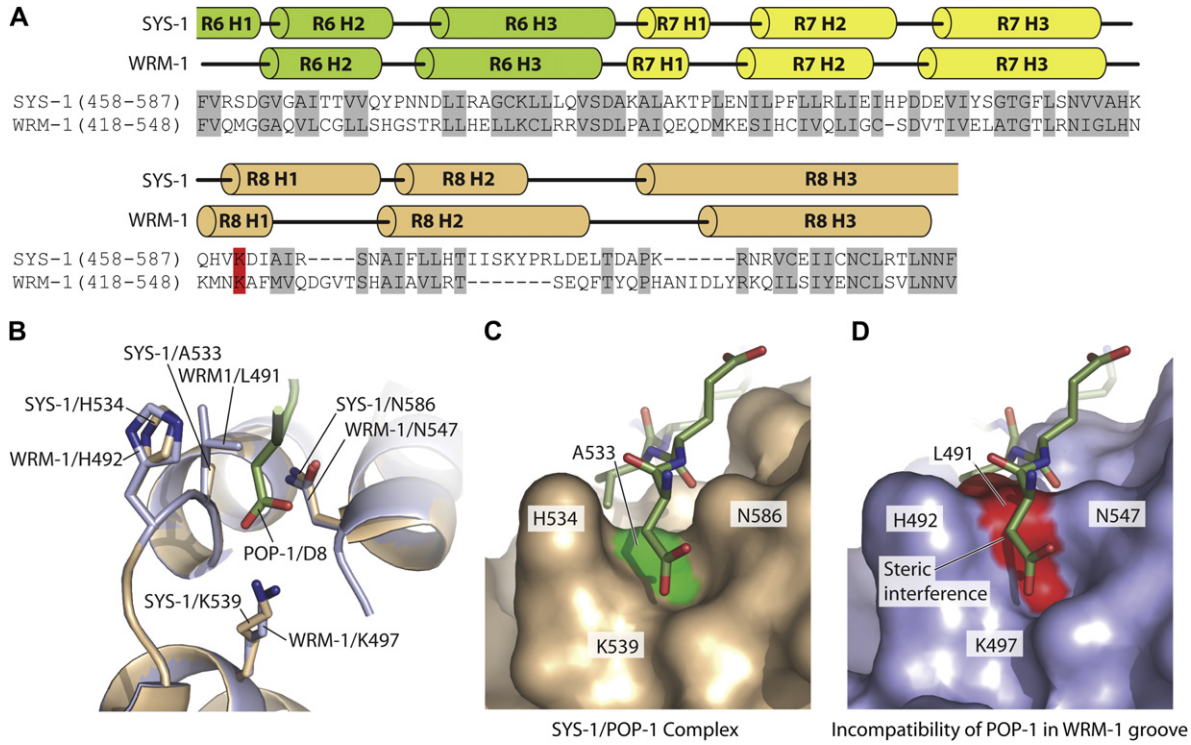

Figure 5. Structural Explanation for the Inability of WRM-1 to Bind POP-1

(A) Secondary structure of R6-R8 of SYS-1 in sequence alignment with corresponding region of WRM-1. Helices are designated by repeat number (e.g., R6) and helix number (e.g., H1).

(B) Superposition of the SYS-1/POP-1 complex together with selected amino acids from the WRM-1 model. The area around the charged button (K539 for SYS-1) is shown. The SYS-1(R6-R8) is shown in tan, WRM-1 corresponding region is in slate, and the POP-1 N-terminal domain is in green.

(C) Structure of the SYS-1/POP-1 complex. SYS-1 surface diagram is shown in tan, with residue A533 in green.

(D) Surface diagram of the WRM-1 model. Residue L491 is shown in red. The fake POP-1 molecule as docked in (B) would collide with the side chain of L491.

with characteristics typical of armadillo repeats. As in canonical β-catenin, each armadillo repeat consists of two or three helices. Once the SYS-1 armadillo repeats were identified, we found that repeats 6–8 were most conserved in both structure and sequence. In addition, the helices of both SYS-1 and canonical β-catenins pack into a superhelical structure with a groove on its surface. The β-catenin binding domain of POP-1 lies along a positively charged region of this SYS-1 groove (this work), much as the β-catenin binding domain of TCF lies along a positively charged region of human β-catenin (Graham et al., 2000, 2001; Poy et al., 2001). Indeed, the similarity of the SYS-1/POP-1 and human β-catenin/TCF interface extends to the conservation of the single lysine-aspartic "charged button" pair that is absolutely conserved in all β-catenin homologs, from *C. elegans* to vertebrates, and that is a critical feature of binding between β-catenin and TCF homologs. In addition to these similarities, the SYS-1 structure also reveals a variety of differences, including a larger superhelical twist, a deeper groove, and more variable armadillo repeats. Therefore, it seems that SYS-1 has retained key aspects of β-catenin function and lost others.

The closest relative of *C. elegans* SYS-1 is *C. elegans* WRM-1, which is the most divergent β-catenin identified by sequence (Korswagen et al., 2000; Rocheleau et al., 1997). Although full length SYS-1 and WRM-1 are only 16% identical (32% similar), a smaller region that corresponds to armadillo repeats 6–8 and that is the critical region for binding POP-1 is 24.5% identical (46% similar). It is highly unlikely that the *C. elegans* β-catenins evolved independently to obtain their armadillo repeat structure and their identical "charged button" consisting of the same amino acids in the same position. Therefore, our results support a model in which a common β-catenin ancestor was duplicated and indeed multiplied in *C. elegans* and that these multiple β-catenins acquired distinct functions during evolution. As previously suggested, BAR-1 retains characteristics of canonical β-catenin, HMP-2 is specialized for adhesion, and WRM-1 evolved a new function to control POP-1/TCF activity (Korswagen, 2002; Cox and Hardin, 2004; Mizumoto and Sawa, 2007). We now add SYS-1, which retains the transcriptional activation function of canonical β-catenin, but appears to be specialized for control of asymmetric cell division. Consistent with that model, SYS-1 clusters together with the other *C. elegans* β-catenins as well as the human canonical β-catenin in the β-catenin clade, when armadillo repeats 6–8 were used to construct the phylogenetic tree. We conclude that SYS-1 is a bona fide member of the β-catenin family.

Structural Basis for Understanding Differential β-Catenin Binding Specificities in *C. elegans*

Our SYS-1 crystal structures and structural models for HMP-2, BAR-1, and WRM-1 provide a basis for predicting how these different *C. elegans* β-catenins achieve their distinct

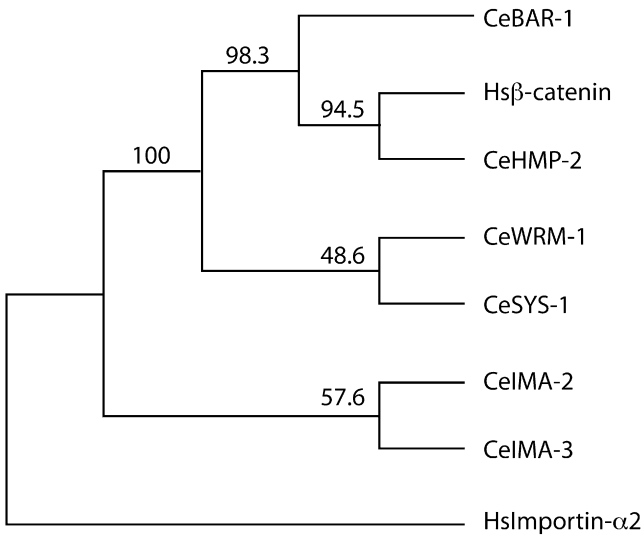

Figure 6. SYS-1 Clusters Phylogenetically with Other β-Catenins
The unrooted neighbor joining tree was derived by PHYLIP using amino acid sequences for armadillo repeats 6–8 of: all four *C. elegans* β-catenins (SYS-1, WRM-1, HMP-2, and BAR-1), human β-catenin, and two *C. elegans* importin-α homologs, IMA-2 and IMA-3. Human importin-α2 was used as an outgroup. One thousand trees were generated and the bootstrap numbers on the branches indicate the percentage of trials the proteins partitioned into the two sets separated by that branch.

protein-binding specificities. This idea can be exemplified by the HMP-2/HMR-1 interaction. Previous structural and biochemical studies showed that armadillo repeats 5–9 of β-catenin form the core binding site for TCF, and this site is also critical for its interaction with E-cadherin (HMR-1 in *C. elegans*) and APC (APR-1 in *C. elegans*) (Graham et al., 2000; Huber and Weis, 2001; Xu and Kimelman, 2007). All of these β-catenin binding partners interact with this same region of β-catenin by means of a conserved $Dx\theta\theta x\Phi x_{2-7}E$ binding motif (θ and Φ are hydrophobic and aromatic residues, respectively), with an almost identical conformation to that first observed in the β-catenin/TCF3 crystal structure (Graham et al., 2000; Xu and Kimelman, 2007). Since POP-1(7–14) also contains this motif and interacts with SYS-1 using a very similar conformation, we predict that HMR-1 uses this motif to interact with HMP-2. The predicted HMP-2 recognition element of HMR-1 is TAPPY**DSLVFFDYE**GS (1194–1209) (Figure 3B).

In vertebrates, two regions in the cadherin cytoplasmic domain are critical for β-catenin/E-cadherin interactions. One is a TCF-like motif discussed above. C-terminal to this motif is the so-called E-cadherin region IV, which contains several Ser/Thr phosphorylation sites (Huber and Weis, 2001). This region is disordered in the β-catenin/E-cadherin complex when unphosphorylated, but interacts extensively with armadillo repeats 3–6 when phosphorylated (Huber and Weis, 2001). The phosphorylation enhances binding of E-cadherin to β-catenin by several hundred-fold and is thus a critical regulatory mechanism of the β-catenin/E-cadherin interaction (Choi et al., 2006). Interestingly, the 20 amino acid (20 aa) repeats of APC also interacts with β-catenin in a phosphorylation-dependent manner that is strikingly similar to region V of the E-cadherin cytoplasmic domain. Comparison of crystal structures of β-catenin/E-cadherin and β-catenin/APC complexes demonstrated that the spacing between the TCF-like motif and phosphorylation-dependent motif is flexible (Kimelman and Xu, 2006). In fact, the corresponding phosphorylated residues in APC and E-cadherin aligned in Figure 3B are in exactly the same spatial position and interact with identical positively charged residues in β-catenin, including K292 and K335 of β-catenin (Table S1). It is very likely that HMR-1, the *C. elegans* E-cadherin, also interacts with HMP-2 in a phosphorylation-dependent manner, with a conformation similar to that of E-cadherin/β-catenin interface. Indeed, all these positively charged residues are conserved between β-catenin and HMP-2 (Table S2), suggesting the HMP-2 groove in armadillo repeats 3–6 can also accommodate a similar phosphorylated motif. In this regard, it should be noted that C-terminal to the TCF-like motif, HMR-1 contains a DxxSxxTxxSxxS sequence that may be sequentially phosphorylated by CK1 in *C. elegans*. CK1 phosphorylates $(pS/T)X_{2-3}(S/T)$ motifs (pS/T indicates phospho-serine or phosphor-threonine, and X can be any residues) (Ferrarese et al., 2007; Meggio and Pinna, 2003; Pulgar et al., 1999).

WRM-1 shows poor POP-1 binding despite having similarity to SYS-1 in the POP-1 binding domain (ARM repeats 6–8). The "charged button" and two of three key nearby residues of WRM-1 (H492 and N547) are conserved and are also consistent with POP-1 binding. However, the third key residue, L491, clashes with POP-1 E9 and a corresponding mutation in SYS-1 (A433L) abolishes the SYS-1/POP-1 interaction (Figure 5). These data highlight the significance of the amino acids near the "charged button" since those neighboring residues must be of the right size to permit formation of the lysine-aspartic salt bridge. Our crystal structures and computational models of structure will serve as the basis for future molecular and biochemical studies of *C. elegans* β-catenins.

A New Model for Identifying Divergent β-Catenins?

The SYS-1 amino acid sequence bears only 9.3% sequence identity to canonical β-catenin, but nonetheless forms armadillo repeats that pack into a superhelical structure similar to canonical β-catenin. This finding means that the current practice of identifying β-catenins, and more generally of identifying armadillo repeat proteins, by sequence comparison is incomplete, and that additional β-catenins remain to be discovered. Currently, two criteria are used to define armadillo repeats: the size of the repeat (~40 residues) and a set of hydrophobic residues in the repeat that are separated by almost fixed spacings. However, SYS-1 defies the first criterion outright and deviates from the second. Thus, 6 out of the 12 SYS-1 armadillo repeats contain over 53 residues, and the longest one has 71 residues. Moreover, the SYS-1 signature hydrophobic residues differ from those of previously identified armadillo repeat proteins (e.g., β-catenin and importin), although these hydrophobic residues pack together in the "3 in 4" mode between neighboring helices, similar to their packing in β-catenin and importin. While the spacings between hydrophobic residues within each helix are similar to previously studied armadillo repeats, the spacings between helices (within and between armadillo repeats) can have very different lengths and therefore are considerably more variable than classical armadillo repeat proteins. The SYS-1 structure therefore calls for revision of the algorithms

used to search for armadillo repeats to allow for more flexible helix lengths and interhelix spacing. Most practical will be a combined structural and functional approach to identify additional armadillo proteins. It is likely that there are many more armadillo repeat or armadillo repeat-like structures in the genome than currently predicted. Among them, new functional β-catenins may be found in vertebrates.

EXPERIMENTAL PROCEDURES

Protein Expression, Purification, and Crystallization

The cDNAs encoding SYS-1(180–811) and POP-1(1–200)/POP-1(1–45) were cloned into pET28a and pGEX-4T1 bacterial expression vectors, respectively. A TEV protease cleavage site was inserted between the affinity tag and the target protein. SYS-1 and POP-1 fusion proteins were overexpressed in the *E. coli* BL21(DE3) strain. For SYS-1, BL21 cells were grown at 25°C overnight after 1 mM IPTG induction. SYS-1 was purified by Ni^{2+}-NTA affinity column (QIAGEN). His-tag was removed by TEV protease and the SYS-1 protein was further purified by a Mono-S column (Pharmacia) and a Superdex S200 gel-filtration column (Pharmacia) equilibrated with 50 mM Tris 8.0, 200 mM NaCl, 16% glycerol, and 3 mM DTT. Eluted protein was concentrated to 5 mg/ml for crystallization. For POP-1, cells were grown for three hours at 37°C after induction with 1 mM IPTG. GST-tagged POP-1 fragments were purified by a glutathione affinity column. After the removal of GST-tag by TEV, POP-1 fragments were further purified by a Mono Q column (Pharmacia). The SYS-1/POP-1 complex was reconstituted by mixing purified SYS-1 and POP-1 at 1:1 molar ratio and further purified by a Superdex 200 column equilibrated with 10 mM Tris 8.5, 50 mM NaCl, 16% glycerol, and 3 mM DTT. The complex was concentrated to ~10 mg/ml for crystallization. Selenomethionyl SYS-1 protein was produced using metabolic inhibition of methionine synthesis as described (Doublie, 1997).

SYS-1 crystals were obtained using the hanging drop vapor diffusion method at 4°C, over a well solution of 100 mM HEPES (pH 6.0), 0.6 M Na/K tartrate, 20 mM glycine, and 5 mM DTT. Selenomethionyl SYS-1/POP-1 complex crystals were obtained using the hanging drop vapor diffusion method at 4°C using a well solution containing 0.3 M Na/K tartrate and 5 mM DTT.

Structural Determination and Refinement

A single-wavelength Se-Met SAD data set of SYS-1/POP-1 was collected at the Advanced Light Source (ALS) beamline 8.2.2. The diffraction data were integrated and scaled with DENZO and SCALEPACK (Otwinowski, 1993; Table 1). The Solve and Resolve programs (Hendrickson, 1991) were used for initial phasing, solvent flattening, density averaging, and automatic model building. Twenty-one out of thirty Se sites in two SYS-1 molecules were located and refined. The resulting figure-of-merit weighted electron density map was readily interpretable (Table 1). The model from RESOLVE was further refined to 2.5 Å resolution using the program Refmac5 (Murshudov et al., 1997). The final model is composed of SYS-1 residues 180–596 and 599–798, POP-1 residues 7–14, and 72 water molecules (Table 1); 94.2% of the amino acids are in the most favorable region of the Ramachandran plot, and none are in outlying regions. The structure of SYS-1 was solved by molecular replacement using the program Amore (Navaza, 1994) with a model derived from the SYS-1/POP-1 complex and refined using Refmac5 (Murshudov et al., 1997). Structure validation was performed using PROCHECK (Laskowski et al., 1993). Electrostatic potential map was calculated by GRASP (Nicholls et al., 1991). The molecular surface was generated with Pymol (Nicholls et al., 1993).

Structure Analysis and Homology Modeling

To analyze the folding of armadillo repeats in SYS-1 (Figure 1C), we did 3D-structure-based sequence alignment using a multiple-alignment version of the structural alignment program MAMMOTH (Ortiz et al., 2002). Pair-wise structure alignment of individual armadillo repeat of SYS-1 and β-catenin was calculated by FAST alignment and search tool (Zhu and Weng, 2005).

To predict the 3D structure of BAR-1, HMP-2, and WRM-1, ClustalW (EBI) was first used to align the protein primary amino acid sequence (Chenna et al., 2003). Then EMBOSS (EBI) was used to score the percentage of identity and similarity of the sequences based alignment (Needleman and Wunsch, 1970). Aligned BAR-1 and HMP-2 armadillo sequences were threaded onto the β-catenin armadillo template backbone, and regions containing insertions or deletions relative to the template were built using an improved version of the Rosetta loop modeling protocol which incorporates CCD closure followed by gradient based energy minimization (Rohl et al., 2004). Side chains were modeled using a combinatorial search through an extended version of the Dunbrack rotamer library supplemented with side-chain conformations from the template using Monte Carlo sampling. WRM-1(418–548) follows the same procedure as above using SYS-1 armadillo repeat (458–587) as template backbone.

Phylogenetic analysis using ClustalW alignments of *C. elegans* and human β-catenins, as well as *C. elegans* and human importin-α proteins, were entered into the PHYLIP package (version 3.67; Felsenstein, 2005) with 1000 bootstrap trials.

GST Pull-Down Assay

Purified GST-POP-1(1–200), POP-1(1–45), POP-1(1–45 D8E) were incubated with 30 μl Glutathione-Sepharose beads (Amersham Pharmacia) for 30 min with gentle rotation at 4°C. The beads were washed three times with 10 mM phosphate buffer (pH 7.4), 500 mM NaCl, 0.1% Triton X-100, 3 mM DTT, and two times with PBS containing 3mM DTT. Purified SYS-1 (either wild-type or mutant) was incubated with the Glutathione-Sepharose beads for 45 min with gentle rotation at 4°C, and then the beads were washed five times with PBS containing 3 mM DTT to remove unbound fractions. The eluted sample was examined by SDS-PAGE. The amounts of purified SYS-1 present for in vitro pull down were determined by UV absorption. The beads incubated with GST were used as a control to detect the nonspecific binding.

ACCESSION NUMBERS

The atomic coordinates and structure factors of SYS-1 and the SYS-1/POP-1 complex have been deposited in the Protein Data Bank, with PDB ID codes 3C2H and 3C2G, respectively.

SUPPLEMENTAL DATA

Supplemental Data include two tables and two figures and can be found with this article online at http://www.developmentalcell.com/cgi/content/full/14/5/751/DC1/.

ACKNOWLEDGMENTS

We thank H. Adam Steinberg for help with figure preparation and E. Haag and L. Adams-Phillips for help with phylogenetic analyses. We are grateful to the staff at ALS beamline 5.0.2 for help with data collection. This work was supported by NIH grant CA90351 to W.X. B.T.P is supported by NIH postdoctoral grant GM75598. J.K. is an investigator of the Howard Hughes Medical Institute.

Received: January 25, 2008
Revised: February 19, 2008
Accepted: February 23, 2008
Published: May 12, 2008

REFERENCES

Aberle, H., Butz, S., Stappert, J., Weissig, H., Kemler, R., and Hoschuetzky, H. (1994). Assembly of the cadherin-catenin complex in vitro with recombinant proteins. J. Cell Sci. *107*, 3655–3663.

Chenna, R., Sugawara, H., Koike, T., Lopez, R., Gibson, T.J., Higgins, D.G., and Thompson, J.D. (2003). Multiple sequence alignment with the Clustal series of programs. Nucleic Acids Res. *31*, 3497–3500.

Choi, H.J., Huber, A.H., and Weis, W.I. (2006). Thermodynamics of β-catenin-ligand interactions: the roles of the N- and C-terminal tails in modulating binding affinity. J. Biol. Chem. *281*, 1027–1038.

Costa, M., Raich, W., Agbunag, C., Leung, B., Hardin, J., and Priess, J.R. (1998). A putative catenin-cadherin system mediates morphogenesis of the *Caenorhabditis elegans* embryo. J. Cell Biol. *141*, 297–308.

Cox, E.A., and Hardin, J. (2004). Sticky worms: adhesion complexes in *C. elegans*. J. Cell Sci. *117*, 1885–1897.

Doublie, S. (1997). Preparation of selenomethionyl proteins for phase determination. Methods Enzymol. *276*, 523–530.

Felsenstein, J. (2005). PHYLIP (Phylogeny Inference Package) version 3.6 (Seattle: Department of Genome Sciences, University of Washington).

Ferrarese, A., Marin, O., Bustos, V.H., Venerando, A., Antonelli, M., Allende, J.E., and Pinna, L.A. (2007). Chemical dissection of the APC Repeat 3 multistep phosphorylation by the concerted action of protein kinases CK1 and GSK3. Biochemistry *46*, 11902–11910.

Gail, R., Frank, R., and Wittinghofer, A. (2005). Systematic peptide array-based delineation of the differential β-catenin interaction with Tcf4, E-cadherin, and adenomatous polyposis coli. J. Biol. Chem. *280*, 7107–7117.

Giles, R.H., van Es, J.H., and Clevers, H. (2003). Caught up in a Wnt storm: Wnt signaling in cancer. Biochim. Biophys. Acta *1653*, 1–24.

Graham, T.A., Weaver, C., Mao, F., Kimelman, D., and Xu, W. (2000). Crystal structure of a β-catenin/Tcf complex. Cell *103*, 885–896.

Graham, T.A., Ferkey, D.M., Mao, F., Kimelman, D., and Xu, W. (2001). Tcf4 can specifically recognize β-catenin using alternative conformations. Nat. Struct. Biol. *8*, 1048–1052.

Hendrickson, W.A. (1991). Determination of macromolecular structures from anomalous diffraction of synchrotron radiation. Science *254*, 51–58.

Herman, M. (2001). *C. elegans* POP-1/TCF functions in a canonical Wnt pathway that controls cell migration and in a noncanonical Wnt pathway that controls cell polarity. Development *128*, 581–590.

Huang, S., Shetty, P., Robertson, S.M., and Lin, R. (2007). Binary cell fate specification during *C. elegans* embryogenesis driven by reiterated reciprocal asymmetry of TCF POP-1 and its coactivator β-catenin SYS-1. Development *134*, 2685–2695.

Huber, A.H., and Weis, W.I. (2001). The structure of the β-catenin/E-cadherin complex and the molecular basis of diverse ligand recognition by β-catenin. Cell *105*, 391–402.

Kidd, A.R., 3rd, Miskowski, J.A., Siegfried, K.R., Sawa, H., and Kimble, J. (2005). A β-catenin identified by functional rather than sequence criteria and its role in Wnt/MAPK signaling. Cell *121*, 761–772.

Kimelman, D., and Xu, W. (2006). β-catenin destruction complex: insights and questions from a structural perspective. Oncogene *25*, 7482–7491.

Korswagen, H.C. (2002). Canonical and non-canonical Wnt signaling pathways in *Caenorhabditis elegans*: variations on a common signaling theme. Bioessays *24*, 801–810.

Korswagen, H.C., Herman, M.A., and Clevers, H.C. (2000). Distinct β-catenins mediate adhesion and signalling functions in *C. elegans*. Nature *406*, 527–532.

Lam, N., Chesney, M.A., and Kimble, J. (2006). Wnt signaling and CEH-22/tinman/Nkx2.5 specify a stem cell niche in *C. elegans*. Curr. Biol. *16*, 287–295.

Laskowski, R.A., MacArthur, M.W., Moss, D.S., and Thronton, J.M. (1993). PROCHECK: A program to check the stereochemical quality of protein structures. J. Appl. Cryst. *26*, 283–291.

Lin, R., Thompson, S., and Priess, J.R. (1995). pop-1 encodes an HMG box protein required for the specification of a mesoderm precursor in early *C. elegans* embryos. Cell *83*, 599–609.

Lin, R., Hill, R.J., and Priess, J.R. (1998). POP-1 and anterior-posterior fate decisions in *C. elegans* embryos. Cell *92*, 229–239.

Logan, C.Y., and Nusse, R. (2004). The Wnt signaling pathway in development and disease. Annu. Rev. Cell Dev. Biol. *20*, 781–810.

Meggio, F., and Pinna, L.A. (2003). One-thousand-and-one substrates of protein kinase CK2? FASEB J. *17*, 349–368.

Miskowski, J., Li, Y., and Kimble, J. (2001). The sys-1 gene and sexual dimorphism during gonadogenesis in *Caenorhabditis elegans*. Dev. Biol. *230*, 61–73.

Mizumoto, K., and Sawa, H. (2007). Cortical β-catenin and APC regulate asymmetric nuclear β-catenin localization during asymmetric cell division in *C. elegans*. Dev. Cell *12*, 287–299.

Moon, R.T., and Kimelman, D. (1998). From cortical rotation to organizer gene expression: toward a molecular explanation of axis specification in *Xenopus*. Bioessays *20*, 536–545.

Moon, R.T., Bowerman, B., Boutros, M., and Perrimon, N. (2002). The promise and perils of Wnt signaling through β-catenin. Science *296*, 1644–1646.

Murshudov, G.N., Vagin, A.A., and Dodson, E.J. (1997). Refinement of macromolecular structures by the maximum-likelihood method. Acta Crystallogr. D Biol. Crystallogr. *53*, 240–255.

Natarajan, L., Witwer, N.E., and Eisenmann, D.M. (2001). The divergent *Caenorhabditis elegans* β-catenin proteins BAR-1, WRM-1 and HMP-2 make distinct protein interactions but retain functional redundancy in vivo. Genetics *159*, 159–172.

Navaza, G. (1994). AMoRe: an automated package for molecular replacement. Acta Crystallogr. A *50*, 157–163.

Needleman, S.B., and Wunsch, C.D. (1970). A general method applicable to the search for similarities in the amino acid sequence of two proteins. J. Mol. Biol. *48*, 443–453.

Nicholls, A., Sharp, K.A., and Honig, B. (1991). Protein folding and association - insights from the interfacial and thermodynamic properties of hydrocarbons. Proteins Struct. Funct. Genet. *11*, 281–296.

Nicholls, A., Bharadwai, R., and Honig, B. (1993). GRASP: Graphical representation and analysis of surface properties. Biophys. J. *64*, A166.

Ortiz, A.R., Strauss, C.E., and Olmea, O. (2002). MAMMOTH (matching molecular models obtained from theory): an automated method for model comparison. Protein Sci. *11*, 2606–2621.

Otwinowski, Z. (1993). Proceedings of the CCP4 Study Weekend: Data Collection and Processing? In Oscillation Reduction Program, N.I.L. Sawyer, and S. Bailey, eds. (Warrington, UK: SERC Daresbury Laboratory), pp. 56.

Peifer, M., and Polakis, P. (2000). Wnt signaling in oncogenesis and embryogenesis–a look outside the nucleus. Science *287*, 1606–1609.

Phillips, B.T., Kidd, A.R., 3rd, King, R., Hardin, J., and Kimble, J. (2007). Reciprocal asymmetry of SYS-1/β-catenin and POP-1/TCF controls asymmetric divisions in *Caenorhabditis elegans*. Proc. Natl. Acad. Sci. USA *104*, 3231–3236.

Polakis, P. (2002). Casein kinase 1: a Wnt'er of disconnect. Curr. Biol. *12*, R499–R501.

Poy, F., Lepourcelet, M., Shivdasani, R.A., and Eck, M.J. (2001). Structure of a human Tcf4-β-catenin complex. Nat. Struct. Biol. *8*, 1053–1057.

Pulgar, V., Marin, O., Meggio, F., Allende, C.C., Allende, J.E., and Pinna, L.A. (1999). Optimal sequences for non-phosphate-directed phosphorylation by protein kinase CK1 (casein kinase-1)–a re-evaluation. Eur. J. Biochem. *260*, 520–526.

Rocheleau, C.E., Downs, W.D., Lin, R., Wittmann, C., Bei, Y., Cha, Y.H., Ali, M., Priess, J.R., and Mello, C.C. (1997). Wnt signaling and an APC-related gene specify endoderm in early *C. elegans* embryos. Cell *90*, 707–716.

Rocheleau, C.E., Yasuda, J., Shin, T.H., Lin, R., Sawa, H., Okano, H., Priess, J.R., Davis, R.J., and Mello, C.C. (1999). WRM-1 activates the LIT-1 protein kinase to transduce anterior/posterior polarity signals in *C. elegans*. Cell *97*, 717–726.

Rohl, C.A., Strauss, C.E., Chivian, D., and Baker, D. (2004). Modeling structurally variable regions in homologous proteins with rosetta. Proteins *55*, 656–677.

Shetty, P., Lo, M.C., Robertson, S.M., and Lin, R. (2005). *C. elegans* TCF protein, POP-1, converts from repressor to activator as a result of Wnt-induced lowering of nuclear levels. Dev. Biol. *285*, 584–592.

Siegfried, K.R., and Kimble, J. (2002). POP-1 controls axis formation during early gonadogenesis in *C. elegans*. Development *129*, 443–453.

Siegfried, K.R., Kidd, A.R., 3rd, Chesney, M.A., and Kimble, J. (2004). The sys-1 and sys-3 genes cooperate with Wnt signaling to establish the proximal-distal axis of the *Caenorhabditis elegans* gonad. Genetics *166*, 171–186.

Thorpe, C.J., Schlesinger, A., and Bowerman, B. (2000). Wnt signalling in *Caenorhabditis elegans*: regulating repressors and polarizing the cytoskeleton. Trends Cell Biol. *10*, 10–17.

van Leeuwen, F., Samos, C.H., and Nusse, R. (1994). Biological activity of soluble wingless protein in cultured *Drosophila* imaginal disc cells. Nature *368*, 342–344.

von Kries, J.P., Winbeck, G., Asbrand, C., Schwarz-Romond, T., Sochnikova, N., Dell'Oro, A., Behrens, J., and Birchmeier, W. (2000). Hot spots in β-catenin for interactions with LEF-1, conductin and APC. Nat. Struct. Biol. *7*, 800–807.

Wodarz, A., and Nusse, R. (1998). Mechanisms of Wnt signaling in development. Annu. Rev. Cell Dev. Biol. *14*, 59–88.

Xu, W., and Kimelman, D. (2007). Mechanistic insights from structural studies of β-catenin and its binding partners. J. Cell Sci. *120*, 3337–3344.

Zhu, J., and Weng, Z. (2005). FAST: a novel protein structure alignment algorithm. Proteins *58*, 618–627.